

SIMULATION OF THE TRANSITION RADIATION TRANSPORT THROUGH AN OPTIC SYSTEM

M. Marongiu^{*1}, A. Mostacci², L. Palumbo², Sapienza University, Rome, Italy

F. Bisesto, E. Chiadroni, G. Di Pirro, G. Franzini, A. Giribono, V. Shpakov,

A. Stella, A. Variola, LNF-INFN, Frascati, Italy

A. Cianchi, Università di Roma II Tor Vergata, Rome, Italy

¹also at LNF-INFN, Frascati, Italy

²also at INFN, Rome, Italy

Abstract

Optical Transition Radiation (OTR) screens are widely used for beam profile measurements. The radiation is emitted when a charged particle beam crosses the boundary between two media with different optical properties. The main advantages of OTR are the instantaneous emission process allowing fast single shot measurements (i.e. bunch by bunch measurements in a multi bunch machine), and the good linearity with the beam charge (if coherent effects can be neglected).

Furthermore, OTR angular distribution strongly depends on beam energy. Since OTR screens are typically placed in several positions along the Linac to monitor beam envelope, one may perform a distributed energy measurement along the machine: this will be useful, for instance, during the commissioning phase of a machine.

This paper deals with the studies of an algorithm to optimize the generation and the transport of the transition radiation through an optic system using the simulation tool Zemax. The algorithm, in combination with a particle tracking code (i.e. Elegant), will allow to simulate the radiation generated by a beam and, so, to take into account beam divergence and energy spread or chromatic effects in the optic system.

INTRODUCTION

In this paper we discuss of an algorithm to optimize the generation and the transport of the transition radiation through an optic system using the simulation tool Zemax. The algorithm, in combination with a particle tracking code (i.e. GPT, Elegant), will allow to simulate the radiation generated by a beam and, so, to take into account beam divergence, correlation and energy spread as well as chromatic effects in the optic system. Indeed, starting from previous work [1, 2], it was possible to improve this simulation tool and make it a reliable source for beam diagnostics simulation.

In a typical monitor setup, the beam is imaged via OTR screen using standard lens optics, and the recorded intensity profile is a measure of the particle beam spot [3]. In conjunction with other accelerator components, it will also be possible to perform various measurements on the beam, namely: its energy and energy spread (with a dipole or corrector magnet), bunch length [4, 5], Twiss parameters [6]

^{*} marco.marongiu@uniroma1.it

(by means of quadrupole scan), Single Shot Emittance [7] (with a microlens array) or in general 6D characterization on bunch phase space [8]. Such technique is common in conventional [9] and unconventional [10–12] high brightness Linacs.

Furthermore, OTR angular distribution strongly depends on beam energy. Since OTR screens are typically placed in several positions along a Linac to monitor beam envelope, one may perform a distributed energy measurement along the machine: this will be useful, for instance, during the commissioning phase of a machine.

TRANSITION RADIATION

Optical Transition Radiation (OTR) screens are widely used for beam profile measurements. The radiation is emitted when a charged particle beam crosses the boundary between two media with different optical properties. For beam diagnostic purposes the visible part of the Transition Radiation is used; an observation geometry in backward direction is chosen corresponding to the reflection of virtual photons at the screen which acts as a mirror.

The main advantages of OTR are the instantaneous emission process allowing fast single shot measurements [13], and the good linearity with the beam charge (if coherent effects can be neglected). The disadvantages are that the process of radiation generation is invasive, and that the radiation intensity is much lower in comparison to scintillation screens. Another advantage of the OTR is the possibility to measure the beam energy from its angular distribution [14, 15].

The angular distribution can be expressed by the well known formula [14]:

$$\frac{dI^2}{d\omega d\Omega} = \frac{e^2}{4\pi^3 c \epsilon_0} \frac{\sin^2 \theta}{\left(\frac{1}{\gamma^2} + \sin^2 \theta\right)^2} R(\omega), \quad (1)$$

where ω is the frequency, Ω is the solid angle, I is the intensity of the radiation, e is the electron charge, γ is the relativistic Lorentz factor, c is the speed of light, ϵ_0 is the vacuum permittivity and $R(\omega)$ is the reflectivity of the screen; the peak of intensity is at $\theta_M = 1/\gamma$ with respect to the beam direction.

Due to the beam divergence, the angular distribution of the whole beam will be different from 0 at the center: assuming a Gaussian distribution of the divergences, the OTR angular

distribution can be written as the convolution between Eq. (1) and the Gaussian distribution as in Eq. (2).

$$I \propto \frac{\sqrt{\pi}\mu}{\nu} \Re \left[\Phi(z) \left(\frac{1}{2} + \mu\nu z \right) \right] - \mu^2, \\ \mu = \frac{1}{\sqrt{2}\sigma'}, \quad \Phi(z) = \frac{1 - \text{erf}(z)}{\exp[-z^2]}, \\ z = \mu(\nu + i\theta), \quad \nu = \frac{1}{\gamma}, \quad (2)$$

where $\text{erf}(z)$ is the complex error function and \Re is the real part [16].

Since for bigger energies the angular distribution narrows, the sensitivity to angular spread is higher than for low energy beams where the angular distribution is wide. Moreover, the beam energy has an impact on the ability of a given optic system to resolve the angular distribution, since the angular distribution narrows as the energy increases; therefore, a change of the optic system (i.e. a bigger focal length) could be necessary while measuring a wide range of beam energies.

ZEMAX SIMULATION

ZEMAX [17] is a widely used software in the optics industry as a standard design tool. It is typically used for lens design and illumination devices.

One has to input to ZEMAX the approximation of the electric field for the OTR induced by a single electron (the so called Single Particle Function SPF) on a target surface [1]:

$$E_h = \frac{e^2}{4\pi^3 \epsilon_0 c} \left[\frac{2\pi}{\gamma\lambda} K_1 \left(\frac{2\pi}{\gamma\lambda} r \right) - \frac{J_0 \left(\frac{2\pi}{\lambda} r \right)}{r} \right] \cos(\phi) \\ E_v = \frac{e^2}{4\pi^3 \epsilon_0 c} \left[\frac{2\pi}{\gamma\lambda} K_1 \left(\frac{2\pi}{\gamma\lambda} r \right) - \frac{J_0 \left(\frac{2\pi}{\lambda} r \right)}{r} \right] \sin(\phi) \quad (3)$$

$$r = \sqrt{(x - x_0)^2 + (y - y_0)^2}$$

$$\phi = \arctan \left(\frac{y - y_0}{x - x_0} \right)$$

with $x - x_0$ and $y - y_0$ the two orthogonal coordinates of the target surface measured from the point of electron incidence (x_0, y_0) , λ is the radiation wavelength, K_1 is the modified Bessel function of first order, and J_0 is the Bessel function of zeroth order. The “h,v” indexes account the horizontal and vertical polarization respectively.

we use the Zemax Programming Languages (ZPL) macro to set a different wavelength for each simulation and to perform a weighted sum of the simulations results in order to take into account changes of quantum efficiency of the used CCD with respect to the wavelength (a typical CCD has its maximum efficiency around a wavelength of 550 nm).

Typically the effects are mitigated by the CCD that acts in a similar way as a filter at 550 nm (green filter): indeed, its quantum efficiency frequency dependence is high at the

550 nm wavelength and goes quickly down at the others frequencies. Figure 1 shows the chromatic effect in case of a full optical spectrum transition radiation.

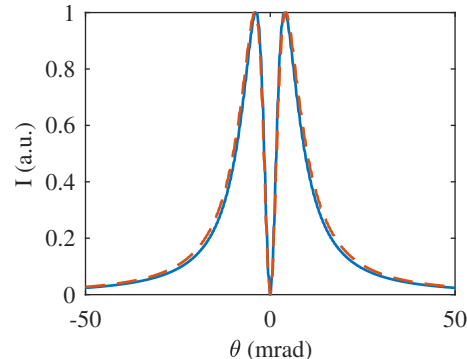


Figure 1: Horizontal profile of the SPF OTR angular distribution for an energy of 123 MeV. The blue continuous line represents the monochromatic simulation, the red dashed line is the polychromatic one.

The ZPL macro can be used also for evaluating the beam divergence and correlation; the ZPL macro takes the output of a particle tracking code (GPT or Elegant) as the input information about the beam distribution (i.e. position, angular momentum and energy of each particle). This method has been experimentally validated [2] with data taken from the SPARC_LAB high brightness electron Linac [9], that was analyzed in [16].

It is of particular interest the possibility to take into account the beam correlation contributions to the emitted radiation; indeed, Eq. 2 is valid only if the beam correlations ($\langle xx' \rangle$, $\langle yy' \rangle$ and $\langle xy \rangle$) are negligible. If we simulate a strongly correlated beam, we obtain an OTR angular distribution different from the theory in the minimum value as can be seen in Fig. 2; the effect of the correlation and of

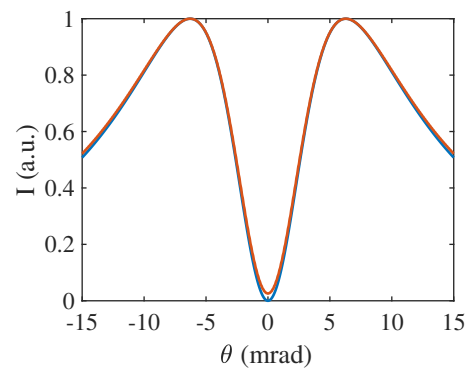


Figure 2: Horizontal profile of the beam angular distribution expected for a 81 MeV beam with a horizontal spot size of 400 μm , a 25 μrad beam divergence and a $\langle xx' \rangle$ correlation of 0.97: the blue continuous line represents the uncorrelated curve (Eq. 2), while the red dashed line is the ZEMAX simulation. The beam correlation and the beam size produce an overall divergence higher than the angular spread taken into account in Eq. 2.

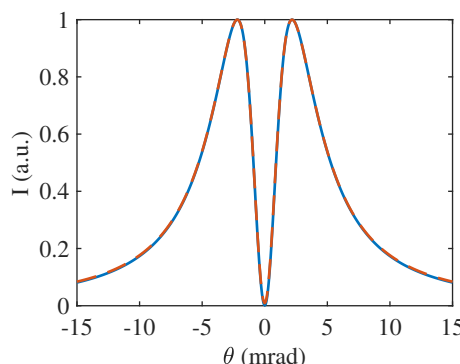


Figure 3: Horizontal profile of the beam angular distribution expected for a 234 MeV beam with a horizontal spot size of 30 μm , a 47 μrad beam divergence and a $\langle xx' \rangle$ correlation of 0.02: the blue continuous line represents the theoretical curve (Eq. 2), while the red dashed line is the ZEMAX simulation. Here, the effects of the correlation and of the beam size are negligible.

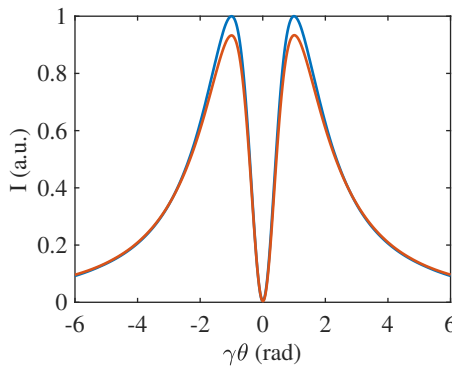


Figure 4: Horizontal profile of the beam angular distribution simulated with ZEMAX at different values of energy spread. The divergence of the beam is 47 μm and its energy is 234 MeV; the blue line represents a beam with an energy spread of 0.1%; the red line represents a beam with 10% energy spread. The peak of intensity tends to decrease with the spread while the lobes gets broader. The position of the peaks is still correctly located at $\theta_M = 1/\gamma$.

the beam size mainly translate in an higher minimum with respect to the theoretical expectation (Eq. 2). On the contrary, a weakly correlated beam does not show this discrepancy as can be seen in Fig. 3; the low value of the correlation gives a negligible contribution to the OTR angular distribution that is hence correctly described by Eq. 2. Both Fig. 2 and Fig. 3 refer to Elegant beam dynamic simulations of the ELI-NP-GBS Linac [18] (soon after the first and the last accelerating module, respectively).

Finally, this macro can evaluate also the impact of the energy spread on the emitted radiation as can be seen in Fig. 4: this is negligible for values up to few percent.

CONCLUSION

It has been shown a simulation model of the Far Field OTR of a typical beam: this model has been previously validated both with the theory and with experimental data.

This model can take advantage of the results of particle tracking code like GPT or Elegant, in order to studies the OTR produced by beams with any transverse phase-space distribution.

The ZPL macro method will be useful also to take into account the effects of a high energy spread on the OTR: this will help, for instance, for plasma accelerated beams [19].

Finally, in combination with a proper optical setup (i.e. a microlens array), this method can be used to evaluate the effects of beam divergence and correlation on the radiation profile.

ACKNOWLEDGMENT

We would like to thank Kevin Cassou and the LAL laboratory for the valuable help.

REFERENCES

- [1] F. G. Bisesto *et al.*, “Zemax simulations describing collective effects in transition and diffraction radiation,” *Optics Express*, vol. 26, no. 4, p. 5075, 2018.
- [2] M. Marongiu *et al.*, “Design of the Diagnostic Stations for the ELI-NP Compton Gamma Source,” in *Proc. 9th International Particle Accelerator Conference (IPAC’18), Vancouver, BC, Canada, April 29-May 4, 2018*, paper WEPAL013, pp. 2173–2176.
- [3] M. Marongiu *et al.*, “Thermal behavior of the optical transition radiation screens for the eli-np compton gamma source,” *Nuclear Instruments and Methods in Physics Research Section A*, 2016.
- [4] D. Filippetto *et al.*, “Phase space analysis of velocity bunched beams,” *Physical Review Special Topics-Accelerators and Beams*, vol. 14, no. 9, p. 092804, 2011.
- [5] R. Pompili *et al.*, “First single-shot and non-intercepting longitudinal bunch diagnostics for comb-like beam by means of electro-optic sampling,” *Nuclear Instruments and Methods in Physics Research Section A: Accelerators, Spectrometers, Detectors and Associated Equipment*, vol. 740, pp. 216–221, 2014.
- [6] A. Mostacci *et al.*, “Chromatic effects in quadrupole scan emittance measurements,” *Physical Review Special Topics-Accelerators and Beams*, vol. 15, no. 8, p. 082802, 2012.
- [7] A. Cianchi *et al.*, “Transverse emittance diagnostics for high brightness electron beams,” *Nuclear Instruments and Methods in Physics Research Section A*, 2016.
- [8] A. Cianchi *et al.*, “Six-dimensional measurements of trains of high brightness electron bunches,” *Physical Review Special Topics-Accelerators and Beams*, vol. 18, no. 8, p. 082804, 2015.
- [9] M. Ferrario *et al.*, “Sparc_lab present and future,” *Nuclear Instruments and Methods in Physics Research Section B*, vol. 309, pp. 183–188, 2013.

[10] P. Antici *et al.*, “Laser-driven electron beamlines generated by coupling laser-plasma sources with conventional transport systems,” *Journal of Applied Physics*, vol. 112, no. 4, p. 044902, 2012.

[11] A. R. Rossi *et al.*, “The external-injection experiment at the sparc_lab facility,” *Nuclear Instruments and Methods in Physics Research Section A*, vol. 740, pp. 60–66, 2014.

[12] R. Pompili *et al.*, “Beam manipulation with velocity bunching for pwfa applications,” *Nuclear Instruments and Methods in Physics Research, Section A*, vol. 829, pp. 17–23, 2016.

[13] G. Marcus *et al.*, “Time-domain measurement of a self-amplified spontaneous emission free-electron laser with an energy-chirped electron beam and undulator tapering,” *Applied Physics Letters*, vol. 101, no. 13, 2012.

[14] V. Ginsburg *et al.*, “Radiation of a uniformly moving electron due to its transition from one medium into another,” *Zhurnal eksperimentalnoi i teoreticheskoi fiziki*, vol. 16, no. 1, pp. 15–28, 1946.

[15] M. Castellano *et al.*, “Analysis of optical transition radiation emitted by a 1 mev electron beam and its possible use as diagnostic tool,” *Nuclear Instruments and Methods in Physics Research Section A*, vol. 357, no. 2, pp. 231–237, 1995.

[16] M. Marongiu *et al.*, “Energy measurements by means of transition radiation in novel linacs,” *Nuclear Instruments and Methods in Physics Research Section A*, 2018, in press.

[17] “Zemax optic studios,” <https://www.zemax.com/products/opticstudio>.

[18] A. Giribono *et al.*, “6d phase space electron beam analysis and machine sensitivity studies for eli-np gbs,” *Nuclear Instruments and Methods in Physics Research Section A*, vol. 829, pp. 274–277, 2016.

[19] M. Ferrario *et al.*, “Eupraxia@sparc_lab: design study towards a compact fel facility at lnf,” *Nuclear Instruments and Methods in Physics Research Section A*, 2018, in press.